Detection of stable positive fixed charges in AlOx activated during annealing with in situ modulated PhotoLuminescence

Pere Roca I Cabarrocas, Anatole Desthieux, Mengkoing Sreng, Pavel Bulkin, Ileana Florea, Etienne Drahi, Barbara Bazer-Bachi, Jean-Charles Vanel, François Silva, Jorge Posada

Version of Record: https://www.sciencedirect.com/science/article/pii/S0927024821002154
Manuscript_604d71717a3226f594d4919809ea0580

Detection of Stable Positive Fixed Charges in AlO_x Activated During Annealing with *In Situ* Modulated PhotoLuminescence

Anatole Desthieux[1,2,3,*], Mengkoing Sreng[2,3], Pavel Bulkin[3], Ileana Florea[3], Etienne Drahi[4,2], Barbara Bazer-Bachi[5], Jean-Charles Vanel[3], François Silva[3], Jorge Posada[1,2], Pere Roca i Cabarrocas[3,2]

1. EDF R&D, Bvd Gaspard Monge, 91120 Palaiseau, France
2. Institut Photovoltaïque d'Ile-de-France (IPVF), 18 Bvd Thomas Gobert, 91120 Palaiseau, France
3. LPICM, CNRS, Ecole Polytechnique, Institut Polytechnique de Paris, route de Saclay, 91128 Palaiseau, France
4. TOTAL GRP, 2 Place Jean Millier – La Défense 6, 92078 Paris La Défense Cedex, France
5. Photowatt, EDF ENR PWT, 33 rue Saint-Honoré, Z.I. Champfleuri, 38300 Bourgoin-Jallieu, France

*. Corresponding author: tel: +33 1 69 86 58 90, email: anatole.desthieux@edf.fr

***Abstract*— An *in situ* Modulated Photoluminescence (MPL) measurement setup mounted on a Plasma Enhanced Chemical Vapor Deposition (PECVD) reactor is described. A method for deriving the actual minority carrier lifetime at a specific injection level of 1.10^{15} cm^{-3} is presented. This tool was used in a case study to monitor the passivation properties of aluminum oxide (AlO_x) thin films upon annealing. Interesting kinetics such as a drop of lifetime at temperatures higher than 250°C along with a recovery of the lifetime during the cooling phase are shown. Moreover, these *in situ* results combined with *ex situ* studies allowed us to demonstrate the formation a stable high positive fixed charge density in the AlO_x layer ($+1.10^{12}$ cm^{-2}), as a consequence of the combination of annealing and light exposure.**

Keywords — In situ, Modulated Photoluminescence, Silicon Solar Cells, Aluminum Oxide, Annealing, Fixed Charges

1. INTRODUCTION

Aluminum oxide (AlO_x) is a widely used material for surface passivation in crystalline silicon (c-Si) solar cells. It is indeed the base material for rear surface passivation in Passivated Emitter and Rear Contact (PERC) cells, and numerous research teams attempt to include it in new solar cell architectures (Tunnel Oxide Passivated Contacts (TOPCon) [1 - 4] or Heterojunction (HJT) [5] solar cells). The application of this material to PV technologies has already been extensively studied over the last decade [6 - 9], and is recently being further pushed towards industrialization by the development of high throughput Atomic Layer Deposition (ALD) techniques [10]. Its outstanding passivation properties are due to a low surface defect density (D_{it}), along with a high negative fixed charge density (Q_f), thus providing a high quality of both chemical and field-effect passivation. In order to achieve this, an annealing step after ALD deposition was shown to be necessary [11 - 13].

Real-time measurements are extremely interesting for the understanding of mechanisms and for process optimization. In order to study the interface quality, the effective minority carrier lifetime is one of the properties most often analyzed, and it has the advantage of being measurable through contactless non-destructive methods. One of them consists in measuring the Modulated Photo-Luminescence (MPL) of a sample which allows a quantitative assessment of the passivation quality.

In this study, we describe a homemade *in situ* MPL acquisition setup that is coupled to a Plasma Enhanced Chemical Vapor Deposition (PECVD) reactor. We describe an approach to determine in real

time the minority carrier lifetime at a minority carrier density of 1.10^{15} cm^{-3}. It is subsequently used to investigate the kinetics of passivation in samples of AlO_x on crystalline silicon during thermal annealing.

2.EXPERIMENTAL SECTION

2.1. Sample fabrication

The substrates used were double-side polished (DSP) n-type (100) float zone (FZ) silicon wafers (100 mm of diameter, 280 µm thick and having a resistivity of approximately 3 Ω.cm) supplied by the wafer manufacturer TOPSIL. Prior to AlO_x deposition, the substrates were cleaned for 30 s in a 5% concentrated hydrofluoric acid (HF) solution for native oxide removal. 9 nm-thick AlO_x films were deposited in a thermal ALD reactor (Picosun) at 150°C with alternative pulses of water vapor and trimethylaluminum (TMA). Samples were subsequently annealed in the PECVD reactor equipped with *in situ* MPL measurement setup described below. The annealing was carried out under 1 Torr of H_2.

2.2. Ex situ characterization techniques

The minority carrier lifetime of samples at the end of the annealing process was measured by the Quasi Steady-State Photo-Conductance technique (Sinton WCT-120). Electron microscopy characterization of synthetized AlO_x thin films (7 nm thick) on c-Si were performed on a Titan-Themis electron microscope operating at 200 kV equipped with a Cs probe corrector with a spatial resolution within nm range using the STEM-HAADF (Scanning Transmission Electron Microscopy-High Angle Annular Dark Field) imaging mode. For all the studied samples cross-section-lamellas have been prepared using a standard lift-out procedure within a Focused Ion Dual beam microscope (FIB, FEI-Scios DualBeam). The fixed charge density Q_f and interface defect density D_{it} of AlO_x thin films were measured by Corona Oxide Characterization On Semiconductor (COCOS) in a PV-2000A tool by Semilab. The Photoluminescence Images were acquired in a "LIS-R2" by BT Imaging.

2.3. In situ Modulated Photoluminescence PECVD reactor

Modulated Photoluminescence (MPL) consists in shining the studied sample with a laser beam of modulated intensity. This results in a modulation of the carrier concentration in the sample at an identical frequency, thus leading to a modulated photoluminescence signal. By measuring the phase shift between this MPL signal and the excitation, the minority carrier lifetime can be determined through the equation [14]:

$$\phi = -\arctan(\omega\tau) \qquad (1)$$

Where ϕ is the aforementioned phase shift, ω the pulsation of the modulation of the laser in $rad.s^{-1}$, and τ the minority carrier lifetime of the sample in s.

The setup developed in this study [15] is an evolution of an *in situ* photoluminescence (PL) system previously described by S. Abolmasov [16]. The PECVD reactor has a grounded electrode with a 9 mm-diameter hole in its center. This electrode is used as a substrate holder, and the hole allows (i) the illumination of the sample in order to photogenerate carriers, and (ii) the MPL signal collection. The illumination source is a laser which delivers a continuous wave beam centered on a wavelength of 785 nm with a spot size corresponding to the full 9 mm-diameter hole aforementioned. The optical power output and modulation frequencies are controlled through a programmable current/temperature controller from Thorlabs. A parabolic mirror was used in order to maximize the collection of the MPL signal. The signal is then converted by an InGaAs photodiode. Finally, the phase shift between the MPL signal and the excitation is measured through a *lock-in* amplifier. This whole setup is schematically represented in Figure 1.

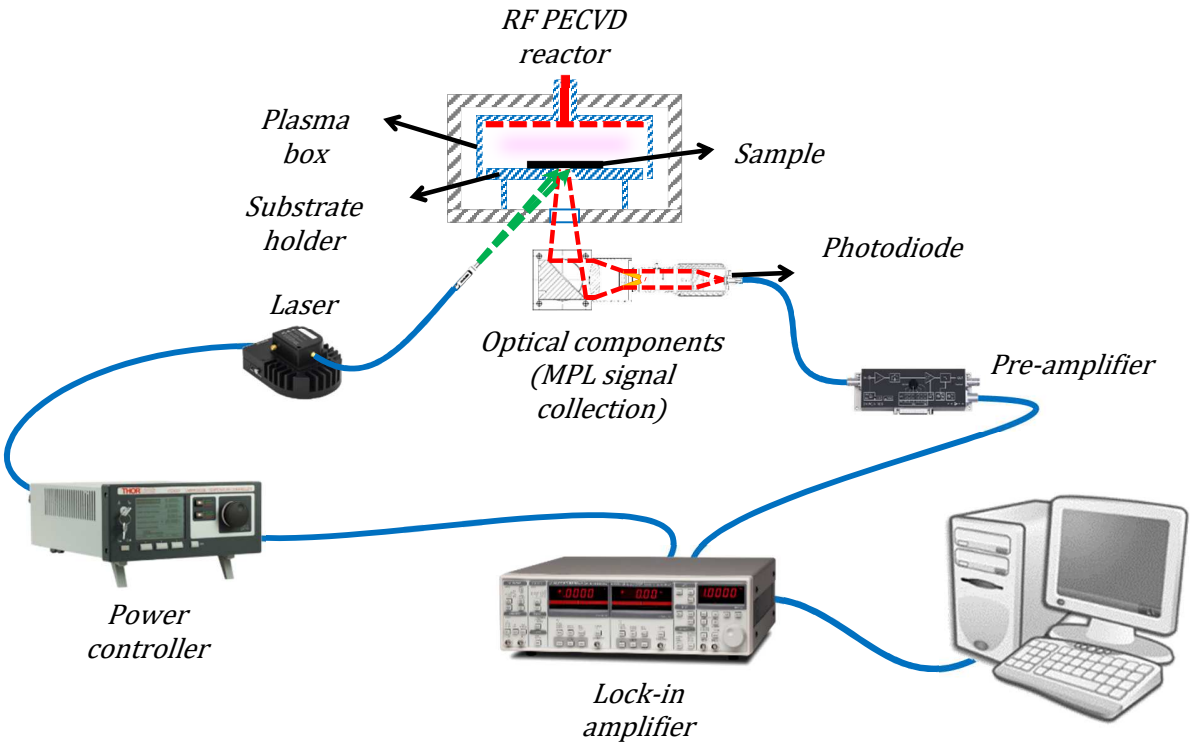

Fig. 1. Schematic representation of the *in situ* MPL acquisition setup coupled with a PECVD reactor [15].

At a given laser power output with a modulation depth of 6%, modulation frequencies ranging from 225 Hz to 625 Hz are used in order to measure various phase shifts and thus get a more reliable fitting for the value of the lifetime in equation (1). This value along with the calculation of the generation rate of photocarriers related to the laser current gives *one value* of τ at a given minority carrier density (represented by one blue dot in Figure 2).

By varying the laser power output and reproducing this series of measurements, it is possible to get a set of lifetime values at their corresponding minority carrier densities. We can finally extrapolate a function for the evolution of τ with the excess minority carrier density (see Figure 2).

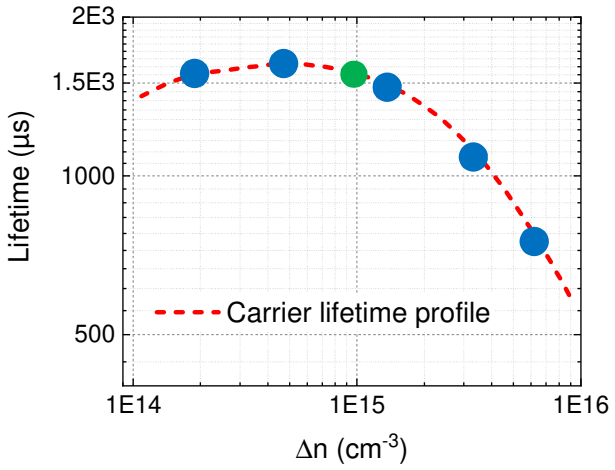

Fig. 2. Various measurements (blue dots) and extrapolation of the function $\tau(\Delta n)$ to derive the minority carrier lifetime at a specific injection level of 1.10^{15} cm^{-3} (green dot) [15].

The lifetime measured by MPL is the differential carrier lifetime, which differs from the effective lifetime measured by QSSPC because of the light bias due to the average intensity of the laser [17]. The effective lifetime can be derived from the equation:

$$\tau_{eff}(G) = \tau_m(G)\left(1 - G\frac{d\tau}{d\Delta n}\Big|_{\Delta n}\right) \qquad (2)$$

Where τ_{eff} is the effective minority carrier lifetime in s, τ_m the (measured) differential minority carrier lifetime in s, G the generation rate in cm^{-3}.s^{-1}, and Δn the injection level in cm^{-3}. During these previous steps, the injection level was assumed to follow the equation $\Delta n = G\tau$. However, since the sample is illuminated only locally, this value may be overestimated (up to 60% for a samples with lifetime of 5 ms).

A lateral diffusion model is thus implemented, solving the differential equation

$$\frac{\partial^2 \Delta n}{\partial x^2} - \frac{1}{D\tau_{eff}}\Delta n = -\frac{G(t,x)}{D} \qquad (3)$$

with D the diffusion coefficient of the excess carriers, estimated at $D = 27$ cm^2.s^{-1}. This allows to iteratively determine – for each time step and each illumination intensity – the excess carrier density profile as well as the lifetime profile in the sample. This results in a new Δn value which takes diffusion into account. This allows to determine the new function $\tau_{eff}(\Delta n)$ with appropriate excess carrier density values. Last but not least, after this correction, it is possible to extract the effective minority carrier lifetime at 1.10^{15} cm^{-3}.

τ_{eff} also depends on temperature, because the bulk lifetime does [18]. In order to take into account for this dependence, the lifetime was assumed to follow a power law [19] given by:

$$\tau_{eff}(T) = \tau_{eff}(300\ K)\left(\frac{T}{300}\right)^{\alpha} \qquad (4)$$

Where T is the temperature in K and α a constant experimentally determined as $\alpha = 1.0026$. This value was measured by annealing at 300°C an n-type FZ wafer provided by Fraunhofer ISE, that was passivated with a SiO_x/(n) poly-Si processed at high temperature (>800°C), and measuring the decrease in lifetime during the cooling phase (see Figure 3). The changes in MPL reflect the evolution of the bulk lifetime. The initial and final lifetimes of the sample have been checked to be identical. Figure 3 shows that the power law of equation (4) describes very well the behavior of the lifetime of the wafer during annealing, with a coefficient of determination $R^2 > 0.99$. We assume the same behavior of the bulk for this sample and for the AlO_x passivated samples in this paper.

This temperature correction is applied to all subsequent data, in order to plot the effective minority carrier lifetime at an equivalent temperature of 300 K, in order to get rid of the contribution of the bulk lifetime, and focus on the evolution of the properties of the passivation layer.

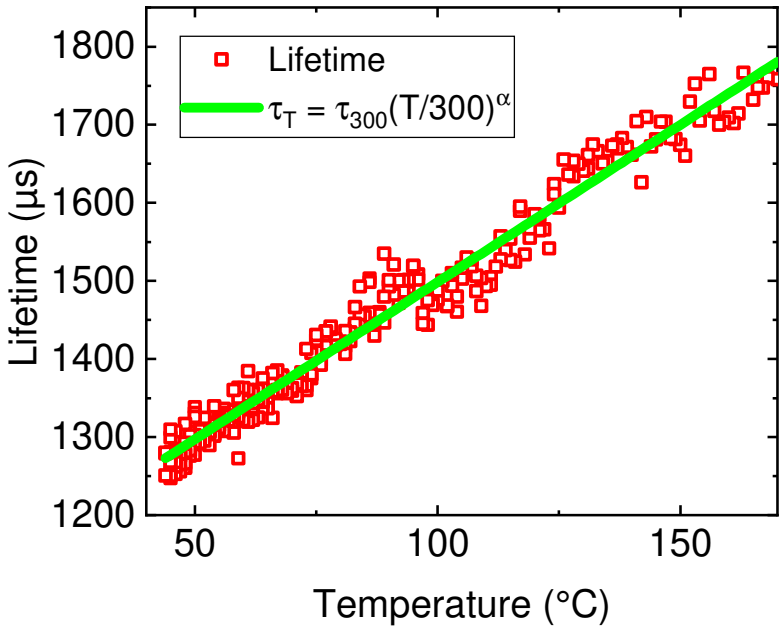

Fig. 3. Evolution with temperature of the minority carrier lifetime of an n-type FZ wafer (1-5 Ωcm) passivated with a SiO_x/(n) poly-Si stack processed at high temperature (> 800°C) during the cooling phase of an annealing at 300°C for 1 minutes in H_2. The green line is the fitting of the lifetime with a power low of coefficient α = 1.0026 (adapted from [15]).

3. Results and Discussion

3.1. In Situ MPL measurements during annealing

In this paper, n-type Float-Zone wafers are used because they show the highest bulk lifetime, which implies that the final lifetime is mostly limited by surface recombination, and therefore allows a good assessment of the passivation quality of the annealed AlO_x layers. The activation of fixed charges in AlO_x still provides high passivation because of the high absolute fixed charge density which induces a strong inversion layer at the interface, thus providing a high field effect passivation.

The standard annealing step that previously showed the best results for our AlO_x passivated samples consists in a 30 min-long plateau at 350°C [9]. Figure 4 shows the evolution of τ_{eff} during such thermal treatment under 1 Torr of H_2. The lifetime starts to increase at the beginning of the heating step, reaching a peak at a temperature of around 250°C ($\tau_{peak} \approx 3.5$ ms). Then, when the temperature further increases, τ_{eff} drops back close to its initial value and stays fairly constant during the 30 minutes of high temperature plateau. Finally, when the sample starts cooling down, the lifetime recovers, and reaches $\tau_{eff} = 3.5$ ms at the end of the annealing step. A measurement of the effective minority carrier lifetime by QSSPC at the end of the process confirms the final value of $\tau_{eff} = 3.2$ ms which is close to the value obtained with the MPL method, thus confirming the validity and accuracy of the different corrections. This kind of kinetics (increase, decrease, low lifetime plateau, recovery) is very reproducible, and was observed on all the samples annealed at 350°C for 30 minutes.

The decrease of lifetime at temperatures higher than 250°C might be due to a loss in chemical passivation. Indeed, this is the temperature at which hydrogen could be starting to effuse and part of the Si-H bonds could be breaking [20]. This could also be a bulk-lifetime-related phenomenon by activating some recombination centers in the FZ silicon wafer [21].

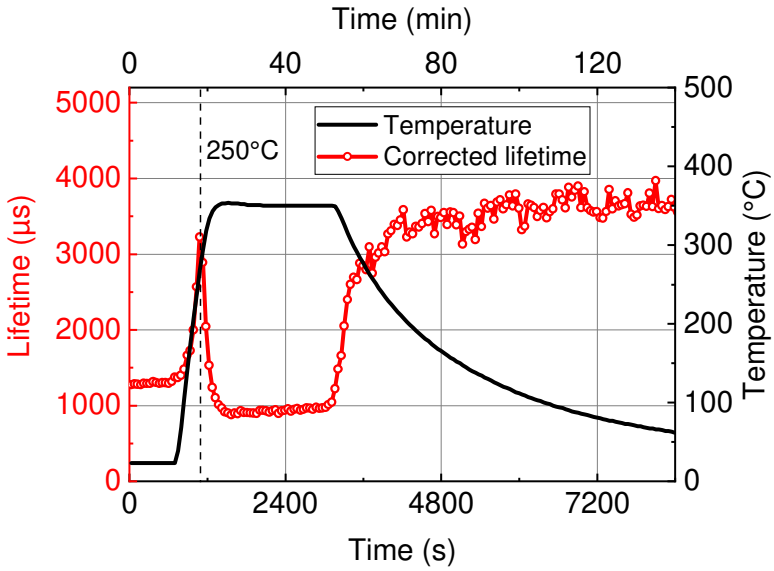

Fig. 4. Evolution of the minority carrier lifetime of an Al_2O_3-passivated c-Si wafer during annealing at 350°C for 30 minutes in H_2. The black curve shows the temperature profile.

The kinetics of passivation shown in Figure 4 raise at least two questions. (1) Since we did not witness any significant change during the 30 min-long plateau, what is the impact of a shorter annealing step? (2) Reaching temperatures up to 350°C seems to be detrimental: what happens if the annealing is stopped at the peak of lifetime: 250°C? In order to answer these questions, two more temperature profiles are investigated: (1) annealing at 350°C for 1 min (Figure 5) and (2) annealing at 250°C for 1 min (Figure 6).

The graph obtained for the one-minute-long annealing at 350°C (Figure 5) shows a similar peak of lifetime at 250°C as in Fig. 3, followed by a drop in lifetime when the temperature is further increased. When the temperature starts to decrease, τ_{eff} starts to increase again, but reaches significantly lower values (2.5 ms) at room temperature than for the thirty-minute-long annealing step.

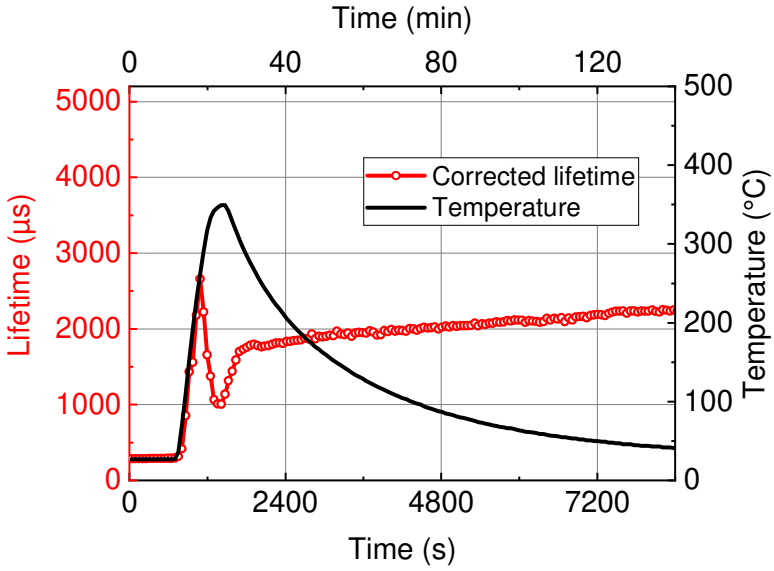

Fig. 5. Evolution of the minority carrier lifetime of an Al_2O_3-passivated c-Si wafer during annealing at 350°C for less than 1 minute in hydrogen environment. The black curve shows the temperature profile.

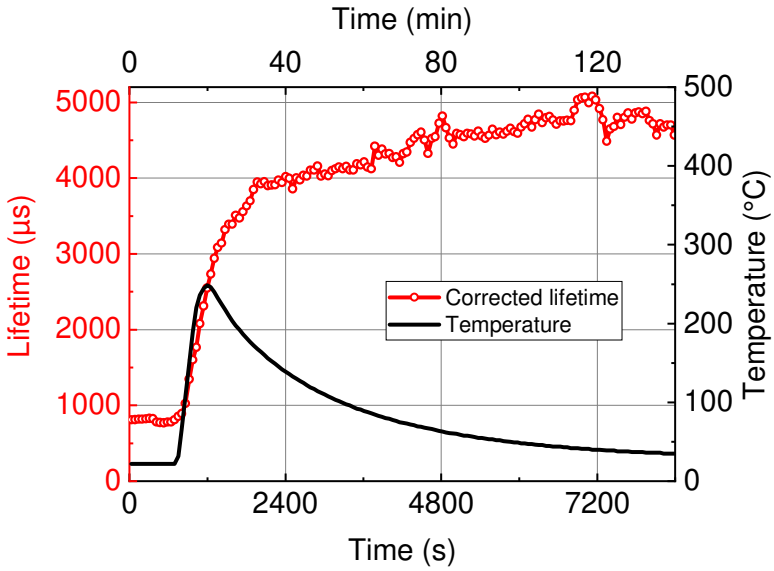

Fig. 6. Evolution of the minority carrier lifetime of an Al_2O_3-passivated c-Si wafer during annealing at 250°C for less than 1 minute in hydrogen environment. The black curve shows the temperature profile.

When the annealing is stopped at 250°C (Fig. 6), the kinetics of the lifetime is significantly different. Indeed, τ_{eff} increases up to 2.5 ms at 250°C, but the lifetime does not decrease afterwards since the temperature does not exceed this threshold value. Surprisingly, τ_{eff} keeps increasing during the cooling phase, reaching 4.7 ms at room temperature, at the end of the MPL measurements. This excellent result shows the importance of *in situ* characterization: it allows to choose specific annealing conditions that otherwise one would not have investigated.

However, the lifetime value measured by QSSPC after the annealing step is significantly different from this last result: only 500 µs. This discrepancy will be investigated further in section 3.4.

3.2. Chemical passivation

One hypothesis to explain the improvement in passivation properties provided by AlO_x thin-films upon annealing is the formation of a thin silicon oxide (SiO_x) layer at the AlO_x/c-Si interface [3,22]. However, in Figure 7 STEM-HAADF images of the c-Si/AlO_x interface show that a thin SiO_x layer is already present in the as-deposited state. The oxide thickness seems to be decreasing with the thermal budget: 1.5 nm for the sample in the as-deposited state, 1 nm for the sample annealed at 250°C for 1 min and 0.8 nm for the sample annealed at 350°C for 30 min. This indicates that the enhancement in passivation is not directly related to the formation of a SiO_x layer at the interface. However, this analysis does not provide information on the passivation quality of the SiO_x thin film: some densification, rearrangements in the Si-O bonds and hydrogen effusion may explain the thinning of the layer and could lead to a change in chemical passivation.

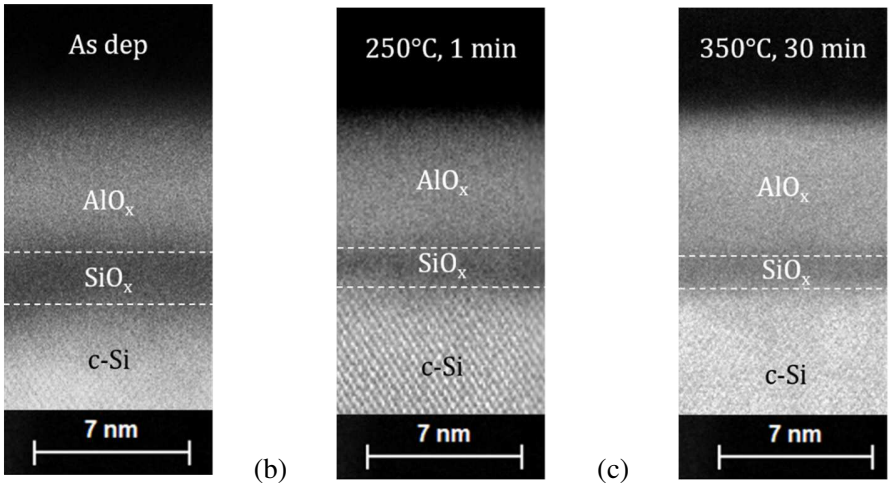

(a) (b) (c)

Fig. 7. STEM-HAADF images of the c-Si/AlO_x interface for (a) the as-deposited sample, (b) the sample annealed at 250°C for 1 min and (c) the one annealed 30 minutes at 350°C

3.3. Field-effect passivation

TABLE I. FIXED CHARGE DENSITY OF ALO_X FILMS AFTER DIFFERENT THERMAL TREATMENTS IN THE PECVD CHAMBER WITH *IN SITU* MPL. DEDUCED FROM CORONA CHARGE EXPERIMENTS.

Annealing	**Fixed charge density Q_f (cm^{-2})**	**Surface defect density D_{it} (cm^{-2})**
350°C for 30 min	$-2.1.10^{12}$	1.10^{11}
350°C for 1 min	$-1.2.10^{12}$	2.10^{11}
250°C for 1 min	$+3.10^{10}$	1.10^{11}

Another important aspect in AlO_x annealing is the activation of fixed charges. Table 1 displays the fixed charge density and the surface defect density in AlO_x thin films for the three samples obtained in section 3.1.

For the sample annealed at 350°C for 30 min, a negative fixed charge density of $-2.1.10^{12}$ cm^{-2} was measured by COCOS. A slightly lower value of $-1.2.10^{12}$ cm^{-2} was obtained after annealing for only 1 min at 350°C. This difference could mean that the annealing step was too short to activate as many fixed charges inside the material, which could have a share in the difference in final minority carrier lifetime value (see Fig. 4 and Fig. 5). For the sample annealed at 250°C for 1 min however, the fixed charge density is $+3.10^{10}$ cm^{-2}. This low absolute value means that the negative fixed charges have not been activated at such low temperature. The absence of charge activation could explain the low final lifetime measured by QSSPC for the sample annealed at 250°C (500 µs), but is not consistent with the high values obtained from the MPL measurement. Despite this large differences in fixed charge densities, the surface defect densities are similar between the different samples, and around 1.10^{11} cm^{-2}.

3.4. Investigation of the discrepancy between QSSPC and MPL

In order to understand the difference between the MPL and QSSPC results, we investigate the homogeneity of the passivation properties; PL images of the samples are shown in Figure 8. It can be seen that for the sample annealed at 350°C for 30 minutes, the PL signal is relatively spatially homogeneous – despite a slightly brighter spot near the center, and damaged areas due to manipulation. On the other hand, the PL image of the sample annealed for 1 min at 250°C shows significant spatial variations. A very bright spot can be noticed at the center of the sample, whereas the rest emits a weaker PL signal in comparison.

This explains the discrepancy noticed between the MPL and QSSPC measurements, since the QSSPC measures the effective minority carrier lifetime on a rather large area (most of the sample) whereas the bright spot corresponds exactly to the area from which the MPL signal is collected.

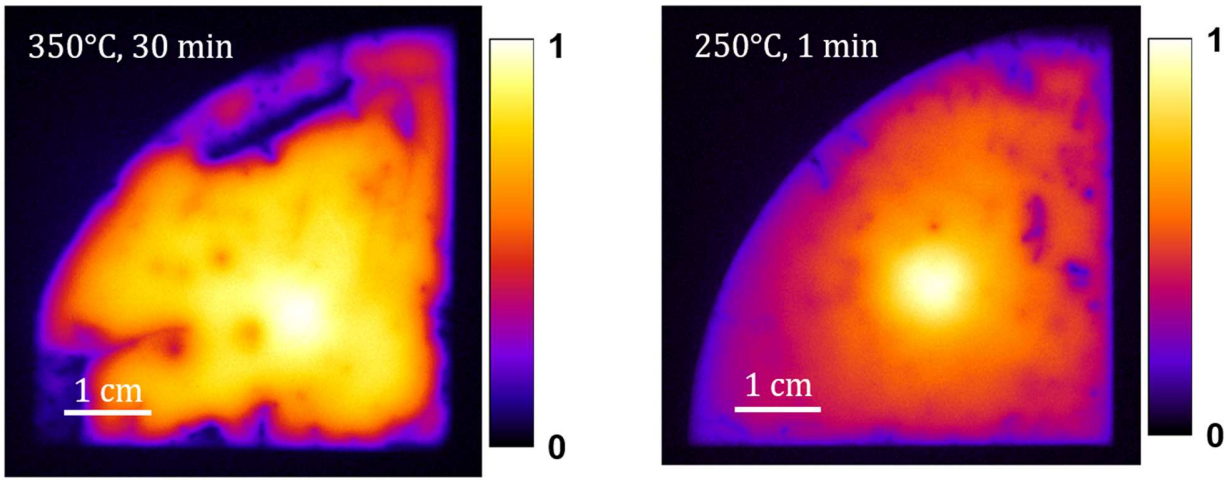

(a) (b)

Fig. 8. PL Images for samples annealed (a) 350°C for 30 min and (b) 250°C for 1 min, using *in situ* MPL during the annealing step.

One hypothesis for this inhomogeneity in the passivation properties is that the charges may have been locally activated by the laser illumination [9,23,24]. In order to investigate this feature, a map of the fixed charge density has been measured on a similar sample (full 100 mm FZ wafer) annealed at 250°C for one minute. The map in Figure 9 shows that the fixed charge density around the spot of high PL signal intensity surprisingly corresponds to a high positive fixed charge density of around $+1.10^{12}$ cm^{-2}. This result has been observed and verified on different samples: in all of them, the fixed charge density reached similar values. D_{it} stays homogeneous at values around 2.10^{-11} cm^{-2}. The high positive fixed charge density is very unusual and mostly witnessed in samples having several nanometers of interface layer of SiO_x or another dielectric [25,26].

This positive fixed charge density could explain the better passivation properties, since the deposition of the AlO_x samples were done on phosphorous doped silicon wafers, so field effect passivation with positive fixed charges is more favorable. As mentioned above, this may not be the only process taking place, since some degradation may be occurring while the temperature gets higher than 250°C.

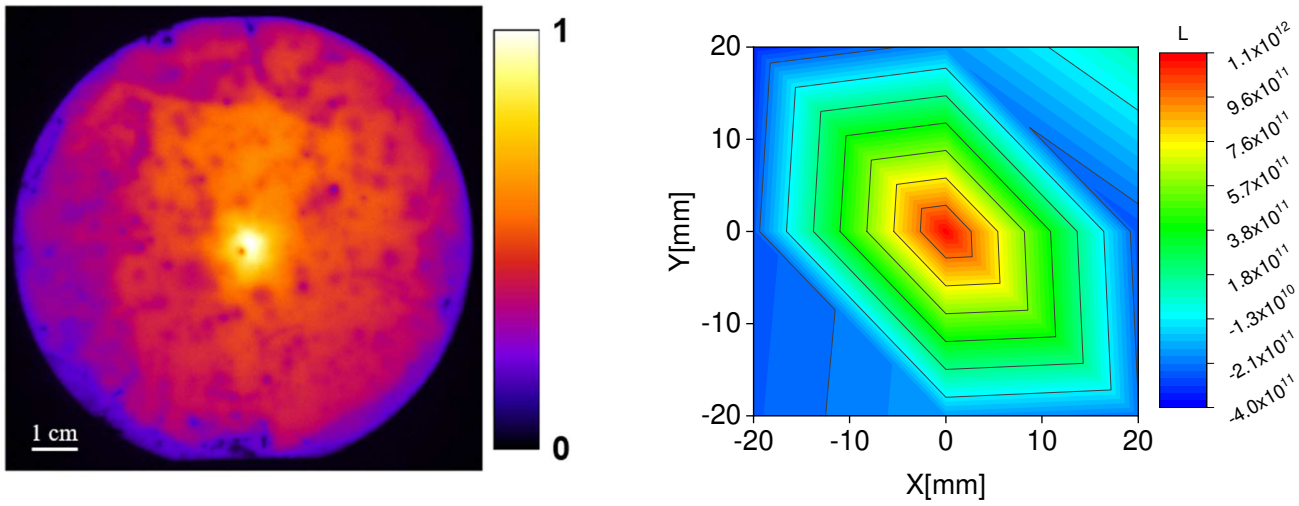

(a) (b)

Fig. 9. (a) PL Image and (b) fixed charge density map for a sample annealed at 250°C for 1 min, using *in situ* MPL during the annealing step.

Additionally, we notice that after 2 months of storage in the dark, the PL images obtained in Figure 8 remain unchanged, which means that the high positive fixed charges are stable, contrarily to reversible negative fixed charge activation through light soaking reported at room temperature [23] .

We showed in this section that the combined action of light and temperature could lead to the formation of a highly passivating AlO_x layer containing a large positive fixed charge density which is stable in time. The annealing under illumination of the full wafer still remains to be investigated. The advantage of such a process is that it only requires the addition of a light source during the annealing step in order to activate fixed charges in AlO_x. The process is simple, low temperature and short, and leads to the formation of very interesting positive fixed charges that are stable in time.

4. SUMMARY

In this study, we have presented an *in situ* MPL setup allowing the measurement in real-time of the minority carrier lifetime at the minority carrier density of 1.10^{15} cm^{-3}. This characterization tool was mounted on a PECVD reactor which gives the possibility to investigate a thermal annealing treatment or a thin-film deposition step. The annealing step following the deposition of an AlO_x passivation layer was studied. The tool allowed to evidence the rich kinetics of the passivation during the annealing. A large drop of lifetime is observed when the sample reaches a temperature greater than 250°C. This spurred the investigation of a faster annealing step at lower temperature (1 min at 250°C instead of 30 min at 350°C). Such a thermal profile allowed to achieve an effective lifetime of 5 ms, but only locally, on the area where the laser used for the MPL measurement was shining the sample. The combined action of light and temperature was shown to activate a high density of fixed charges, which were both positive and stable. This could lead to an additional interest in the use of AlO_x for passivating both n-type and p-type semiconductors. This study shows that annealing under illumination could have the ability to provide a simple and fast way to get positively charged AlO_x layers. We are currently investigating the addition of a light source to shine the whole sample during the thermal annealing.

CREDIT AUTHORSHIP CONTRIBUTION STATEMENT

Anatole Desthieux: Conceptualisation, Investigation, Validation, Visualisation, Writing – Orignal Draft, Writing – Review & Editing. **Mengkoing Sreng**: Conceptualisation, Investigation, Software, Visualisation. **Pavel Bulkin**: Resources. **Ileana Florea**: Investigation. **Etienne Drahi**: Supervision. **Barbara Bazer-Bachi**: Supervision. **Jean-Charles Vanel**: Supervision, Resources, Software. **François**

Silva: Supervision, Conceptualisation, Funding acquisition. **Jorge Posada**: Supervision, Funding acquisition. **Pere Roca i Cabarrocas**: Supervision, Project administration, Writing – Review & Editing.

DECLARATION OF COMPETING INTEREST

The authors declare that they have no known competing interests or personal relationships that could have appeared to influence the work reported in this paper.

ACKNOWLEDGMENT

The authors acknowledge the support from the BEER team from LPICM for technical support in building the *in situ* MPL setup, and thank the team Bivour from Fraunhofer ISE for providing the SiO_x/poly-Si passivated samples. Funding: this work was supported by the French National Research and Technology Agency (ANRT-CIFRE 2018/1033 – PhD thesis of Anatole Desthieux) and by the French National Research Agency (Programme d'Investissement d'Avenir – ANR-IEED-002-01 & 10-EQPX-50, pole NanoTEM and Centre Interdisciplinaire de Microscopie Electronique de l'X – CIMEX).

REFERENCES

[1] C. Hollemann, F. Haase, J. Krügener, Firing stability of n-type poly-Si on oxide junctions formed by quartz tube annealing, (2020) 5.

[2] C.-H. Hsu, C.-W. Huang, Y.-S. Cho, W.-Y. Wu, D.-W. Wuu, X.-Y. Zhang, W.-Z. Zhu, S.-Y. Lien, C.-S. Ye, Efficiency improvement of PERC solar cell using an aluminum oxide passivation layer prepared via spatial atomic layer deposition and post-annealing, Surface and Coatings Technology. (2018). doi:10.1016/j.surfcoat.2018.12.016.

[3] G. Kaur, N. Dwivedi, X. Zheng, B. Liao, L.Z. Peng, A. Danner, R. Stangl, C.S. Bhatia, Understanding Surface Treatment and ALD AlOx Thickness Induced Surface Passivation Quality of c-Si Cz Wafers, IEEE Journal of Photovoltaics. 7 (2017) 1224–1235. doi:10.1109/JPHOTOV.2017.2717040.

[4] B.W.H. van de Loo, B. Macco, M. Schnabel, M.K. Stodolny, A.A. Mewe, D.L. Young, W. Nemeth, P. Stradins, W.M.M. Kessels, On the hydrogenation of Poly-Si passivating contacts by Al2O3 and SiN thin films, Solar Energy Materials and Solar Cells. 215 (2020) 110592. doi:10.1016/j.solmat.2020.110592.

[5] D. Tröger, M. Grube, J. Lehnert, T. Mikolajick, Al2O3-TiOx as full area passivating contacts for silicon surfaces utilizing oxygen scavenging titanium interlayers, Solar Energy Materials and Solar Cells. 215 (2020) 110651. doi:10.1016/j.solmat.2020.110651.

[6] G. Dingemans, W.M.M. Kessels, Status and prospects of Al2O3 -based surface passivation schemes for silicon solar cells, Journal of Vacuum Science & Technology A: Vacuum, Surfaces, and Films. 30 (2012) 040802. doi:10.1116/1.4728205.

[7] B. Liao, R. Stangl, F. Ma, T. Mueller, F. Lin, A.G. Aberle, C.S. Bhatia, B. Hoex, Excellent c-Si surface passivation by thermal atomic layer deposited aluminum oxide after industrial firing activation, Journal of Physics D: Applied Physics. 46 (2013) 385102. doi:10.1088/0022-3727/46/38/385102.

[8] E. Simoen, A. Rothschild, B. Vermang, J. Poortmans, R. Mertens, A Deep-Level Transient Spectroscopy Comparison of the SiO2/Si and Al2O3/Si Interface States, ECS Transactions. 41 (2019) 37–44. doi:10.1149/1.3628607.

[9] F. Lebreton, Silicon surface passivation properties of aluminum oxide grown by atomic layer deposition for low temperature solar cells processes, phdthesis, Université Paris-Saclay, 2017.

[10] J. Melskens, B.W.H. van de Loo, B. Macco, M.F.J. Vos, J. Palmans, S. Smit, W.M.M. Kessels, Concepts and prospects of passivating contacts for crystalline silicon solar cells, in: IEEE, 2015: pp. 1–6. doi:10.1109/PVSC.2015.7355646.

[11] G. Dingemans, P. Engelhart, R. Seguin, F. Einsele, B. Hoex, M.C.M. van de Sanden, W.M.M. Kessels, Stability of Al2O3 and Al2O3/a-SiNx:H stacks for surface passivation of crystalline silicon, Journal of Applied Physics. 106 (2009) 114907. doi:10.1063/1.3264572.
[12] K. Arafune, S. Miki, R. Matsutani, J. Hamano, H. Yoshida, T. Tachibana, H.J. Lee, A. Ogura, Y. Ohshita, S.-I. Satoh, Surface Recombination of Crystalline Silicon Substrates Passivated by Atomic-Layer-Deposited AlOx, Japanese Journal of Applied Physics. 51 (2012) 04DP06. doi:10.1143/JJAP.51.04DP06.
[13] J.A. Töfflinger, A. Laades, C. Leendertz, L.M. Montañez, L. Korte, U. Stürzebecher, H.-P. Sperlich, B. Rech, PECVD-AlOx/SiNx Passivation Stacks on Silicon: Effective Charge Dynamics and Interface Defect State Spectroscopy, Energy Procedia. 55 (2014) 845–854. doi:10.1016/j.egypro.2014.08.068.
[14] R. Brüggemann, S. Reynolds, Modulated photoluminescence studies for lifetime determination in amorphous-silicon passivated crystalline-silicon wafers, Journal of Non-Crystalline Solids. 352 (2006) 1888–1891. doi:10.1016/j.jnoncrysol.2005.11.092.
[15] M. Sreng, Development of in-situ photoluminescence characterization tools for the real-time study of semiconductor materials for photovoltaic application, IPParis, 2019.
[16] S.N. Abolmasov, P. Roca i Cabarrocas, In situ photoluminescence system for studying surface passivation in silicon heterojunction solar cells, Journal of Vacuum Science & Technology A: Vacuum, Surfaces, and Films. 33 (2015) 021201. doi:10.1116/1.4902014.
[17] J.A. Giesecke, S.W. Glunz, W. Warta, Understanding and resolving the discrepancy between differential and actual minority carrier lifetime, Journal of Applied Physics. 113 (2013). doi:10.1063/1.4790716.
[18] S. Bernardini, T.U. Naerland, A.L. Blum, G. Coletti, M.I. Bertoni, Unraveling bulk defects in high-quality c-Si material via TIDLS: Unraveling bulk defects in high-quality c-Si material, Progress in Photovoltaics: Research and Applications. 25 (2017) 209–217. doi:10.1002/pip.2847.
[19] P.C. Mathur, R.P. Sharma, P. Saxena, J.D. Arora, Temperature dependence of minority carrier lifetime in single-crystal and polycrystalline Si solar cells, Journal of Applied Physics. 52 (1981) 3651–3654. doi:10.1063/1.329101.
[20] J.C. Goverde, Characterization and optimization of aluminum oxide films as p-type Czochralski silicon passivation layer, Master's thesis, TU Delft, 2012.
[21] N.E. Grant, V.P. Markevich, J. Mullins, A.R. Peaker, F. Rougieux, D. Macdonald, J.D. Murphy, Permanent annihilation of thermally activated defects which limit the lifetime of float-zone silicon: Permanent annihilation of thermally activated defects in FZ-Si, Physica Status Solidi (A). 213 (2016) 2844–2849. doi:10.1002/pssa.201600360.
[22] V. Naumann, M. Otto, R.B. Wehrspohn, C. Hagendorf, Chemical and structural study of electrically passivating Al2O3/Si interfaces prepared by atomic layer deposition, Journal of Vacuum Science & Technology A: Vacuum, Surfaces, and Films. 30 (2012) 04D106. doi:10.1116/1.4704601.
[23] B. Liao, R. Stangl, T. Mueller, F. Lin, C. Bhatia, B. Hoex, The effect of light soaking on crystalline silicon surface passivation by atomic layer deposited Al2O3, Journal of Applied Physics. 113 (2013) 024509. doi:10.1063/1.4775595.
[24] F. Lebreton, R. Lachaume, P. Bulkin, F. Silva, S.A. Filonovich, E.V. Johnson, P. Roca i Cabarrocas, Deleterious electrostatic interaction in silicon passivation stack between thin ALD Al2O3 and its a-SiNx:H capping layer: numerical and experimental evidences, Energy Procedia. 124 (2017) 91–98. doi:10.1016/j.egypro.2017.09.328.
[25] G. Dingemans, N.M. Terlinden, M.A. Verheijen, M.C.M. van de Sanden, W.M.M. Kessels, Controlling the fixed charge and passivation properties of Si(100)/Al2O3 interfaces using ultrathin SiO2 interlayers synthesized by atomic layer deposition, Journal of Applied Physics. 110 (2011) 093715. doi:10.1063/1.3658246.
[26] N.M. Terlinden, G. Dingemans, V. Vandalon, R.H.E.C. Bosch, W.M.M. Kessels, Influence of the SiO2 interlayer thickness on the density and polarity of charges in Si/SiO2/Al2O3 stacks as studied

by optical second-harmonic generation, Journal of Applied Physics. 115 (2014) 033708. doi:10.1063/1.4857075.